Adiabatic *N*-soliton interactions of Bose-Einstein condensates in external potentials

V. S. Gerdjikov,[1,*] B. B. Baizakov,[2,†] M. Salerno,[2,‡] and N. A. Kostov[3,§]

[1]*Institute for Nuclear Research and Nuclear Energy, Bulgarian Academy of Sciences, Blvd. Tzarigradsko chaussee 72, 1784 Sofia, Bulgaria*

[2]*Dipartimento di Fisica "E.R. Caianiello" and Consorzio Nazionale, Interuniversitario per le Scienze Fisiche della Materia (CNISM), Unitá di Salerno, Universitá di Salerno, via S. Allende, I84081 Baronissi (SA), Italy*

[3]*Institute for Electronics, Bulgarian Academy of Sciences, Blvd. Tzarigradsko chaussee 72, 1784 Sofia, Bulgaria*

(Received 5 December 2005; published 13 April 2006)

A perturbed version of the complex Toda chain (CTC) has been employed to describe adiabatic interactions within an *N*-soliton train of the nonlinear Schrödinger equation. Perturbations induced by weak quadratic and periodic external potentials are studied by both analytical and numerical means. It is found that the perturbed CTC adequately models the *N*-soliton train dynamics for both types of potentials. As an application of the developed theory, we consider the dynamics of a train of matter-wave solitons confined to a parabolic trap and optical lattice, as well as tilted periodic potentials. In the last case, we demonstrate that there exist critical values of the strength of the linear potential for which one or more localized states can be extracted from a soliton train. An analytical expression for these critical strengths for expulsion is also derived.

DOI: 10.1103/PhysRevE.73.046606 PACS number(s): 42.65.Tg, 03.75.Lm, 45.20.Jj

I. INTRODUCTION

One of the most remarkable phenomena occurring in nonlinear systems is the possibility to form localized states of a soliton type as a result of the interplay between dispersion and nonlinearity. These states display interesting properties in response to external fields and their interactions have been the subject of continuous interest since the creation of the soliton theory. Besides the motivation from the viewpoint of fundamental physics, studies on soliton interactions are very important for applications such as optical fiber communications systems, where optical solitons are used as information bit carriers [1]. In this context, the interaction between neighboring solitons in a train limits the transmission capacity of the communication system, so that soliton interaction becomes very important for optimal information packing and transmission rates design. Trains of solitons (fluxons) in interaction play an important role also in long Josephson junctions where their dynamics, induced by external magnetic fields, is used to construct flux-flow oscillators of interest for applications in superconducting mm and sub-mm wave electronics [2]. Other rapidly developing fields in which interacting solitons play a crucial role are photonic crystals [3] and Bose-Einstein condensates (BEC) [4].

Recently, BEC solitons have attracted a great deal of interest both from the theoretical and the experimental point of view (see, e.g., Ref. [5]). In particular, self-trapped states capable of propagating in space without distortion are of interest for pulsed atomic soliton lasers, atomic nanolitography, and high-precision interferometry [6], and the transport of BEC solitons in the presence of external potentials, serving as magnetic and optical traps and waveguides, may become important in future technologies.

The aim of the present paper is to study the adiabatic dynamics of a train of *N* interacting solitons of the nonlinear Schrödinger equation (NLS) in weak external potentials. As a physical model, we consider matter-wave solitons in quasi-one-dimensional BEC with attractive interactions between atoms, such as ^{7}Li, ^{87}Rb, or ^{137}Cs. The results, however, are of interest also for nonlinear optics and for photonic crystals. In particular, we study the *N*-soliton dynamics in parabolic, linear, and periodic potentials, modeling the NLS train soliton interaction in terms of a complex Toda chain (CTC) which is valid in the adiabatic approximation. This model has been successfully used in previous papers (see Refs. [7–12]) and will be used here to continue the analysis in [13,14] on the perturbed CTC (PCTC) as a model for *N*-soliton interaction in BEC with quadratic and periodic potentials. Our results provide an additional confirmation of the stabilization properties of the periodic potentials observed in [15,16] in a different physical setup. In particular, for the case of an *N*-soliton train trapped in a weak parabolic trap, we find that the train performs contracting and expanding oscillations if its center of mass coincides with the minimum of the potential, while it oscillates around the minimum of the potential as a whole if its center of mass is shifted from the minimum. In the last case, contracting and expanding motions of the soliton train are superimposed to the center of mass dynamics. As the strength of the parabolic trap increases, we find from numerical simulations that the *N*-soliton dynamics becomes more complicated with the merging (splitting) of individual solitons when the train is contracted (expanded) during its oscillating motion in the trap. This behavior resemble the phenomenon of "missing solitons" observed in the experiment [17].

We have investigated the case of a tilted periodic potentials, i.e., a potential which is the superposition of periodic and linear potentials. The effect of the linear potential, if it is strong enough, is that it can overcome the stabilization effect

*Email address: gerjikov@inrne.bas.bg
†Email address: baizakov@sa.infn.it
‡Email address: salerno@sa.infn.it
§Email address: nakostov@ie.bas.bg

of the periodic potential. As a result, we show that there exist critical values of the strength of the linear potential for which one or more localized states can be extracted from a soliton train (array). We find that the critical strength for expulsion changes with the number of the solitons in the train. In this regard we have derived an analytical expression for the potential critical strengths at which expulsion is achieved by means of a Hamiltonian approach for the PCTC. From this comparison, we find that the analysis based on the PCTC provides a good description for the expulsion phenomena.

We remark that since the critical value of the potential strength is an indirect measure of the binding energy of an N-solitons train, one could use BEC soliton arrays in accelerated optical lattices to measure N-solitons matter-wave binding energies. One could indeed reproduce the effect of the linear potential by means of accelerated optical lattices and measuring the critical acceleration at which the expulsion of one soliton from the array occurs. We hope experiments in this direction will be performed soon.

The paper is organized as follows. In Sec. II we introduce the mean field Gross-Pitaevskii equation (GPE) appropriate for quasi-one-dimensional BEC in external potentials and discuss the N-soliton interaction in terms of the complex Toda chain. In Sec. III we study the perturbed nonlinear Schrödinger equation and the perturbed CTC equation in the adiabatic approximation for different types of external potentials: quadratic, linear, and periodic. The analysis of the N-soliton dynamics obtained from the perturbed CTC with the above potentials is compared with direct numerical GPE simulations in Sec. IV. In Sec. V we introduce a Hamiltonian formulation of the PCTC and derive an analytical expression for the critical strengths of the linear potential for which the phenomenon of soliton expulsion occurs. Finally, in the last section the main results of the paper are briefly summarized.

II. MODEL EQUATIONS AND N-SOLITON INTERACTION

The dynamics of a condensate in the mean field approximation at zero temperature is governed by the 3D nonlinear Schrödinger equation [in the BEC context called also as Gross-Pitaevskii equation (GPE)]

$$i\hbar\frac{\partial\Psi}{\partial t}=\left[-\frac{\hbar^2}{2m}\nabla^2+V(x,y,z)+\frac{4\pi\hbar^2 a_s\mathcal{N}}{m}|\Psi|^2\right]\Psi, \tag{2.1}$$

where $\Psi(\mathbf{r},t)$ is the macroscopic wave function of the condensate normalized so that $\int|\Psi(\mathbf{r})|^2 d\mathbf{r}=1$, $\mathcal{N}$ is the total number of atoms, m is the atomic mass, a_s is the s-wave scattering length (below we shall be concerned with attractive BEC for which $a_s<0$), and

$$V(x,y,z)=\frac{m}{2}[\omega_x^2x^2+\omega_\perp^2(y^2+z^2)] \tag{2.2}$$

is the axially symmetric trapping potential which provides for the tight confinement in the transverse plane (y,z), as compared to loose axial trapping, assuming $\omega_x^2/\omega_\perp^2\ll 1$. The condensate trapped in such a potential acquires a highly elongated form.

When the transverse confinement is strong enough, so that the transverse oscillation quantum is much greater than the characteristic mean-field interaction energy

$$\hbar\omega_\perp \gg (4\pi\hbar^2|a_s|/m)\mathcal{N}|\Psi|^2, \tag{2.3}$$

the dynamics is effectively one-dimensional. In this case, the wave function may be factorized as $\Psi(x,y,z,t)=\psi(x,t)\phi(y,z)$, where $\phi(y,z)=\exp[-(y^2+z^2)/2a_\perp^2]/\sqrt{\pi}a_\perp$ is the normalized ground state of the 2D harmonic oscillator in the transverse direction, with $a_\perp=\sqrt{\hbar/m\omega_\perp}$ being the corresponding transverse harmonic-oscillator length. Note that, by estimating the matter-wave density as $\mathcal{N}|\Psi|^2\sim\mathcal{N}/(\pi a_\perp^2 a_x)$, the condition (2.3), which ensures decoupling of the transverse and longitudinal modes of the condensate, can be written as $\mathcal{N}|a_s|/a_x\ll 0.25$. On the other hand, the critical number of atoms for collapse of an attractive BEC in a cylindrically symmetric trap was given in [18] as $\mathcal{N}_{\rm cr}=\kappa a_x/|a_s|$, with κ a dimensionless constant which depends on the trap aspect ratio $\lambda=\omega_x/\omega_\perp$. For $\lambda=1/100$ it was found that $\kappa=0.314$ [18], so that the condition for avoiding collapse $\mathcal{N}<\mathcal{N}_{\rm cr}$ (i.e., $\mathcal{N}|a_s|/a_x<\kappa$) is automatically satisfied if inequality (2.3) is valid. Inserting the factorized expression into the 3D GPE (2.1), and integrating it over the transverse plane (y,z), one derives the effective 1D equation

$$i\hbar\frac{\partial\psi}{\partial t}=\left[-\frac{\hbar^2}{2m}\frac{\partial^2}{\partial x^2}+\frac{m}{2}\omega_x^2x^2+g_{\rm 1D}\mathcal{N}|\psi|^2\right]\psi, \tag{2.4}$$

where we have neglected the zero-point energy of the transverse motion, $\hbar\omega_\perp$, and defined a coefficient of the 1D nonlinearity, $g_{\rm 1D}=4\pi\hbar^2 a_s m^{-1}\int|\phi(y,z)|^4 dydz=2a_s\hbar\omega_\perp$. It is convenient to use normalized units for time and space variables, introducing transformations $t\to\omega_\perp t$, $x\to x/a_\perp$, and the rescaled wave function $u\to\sqrt{2\mathcal{N}|a_s|}\psi$,

$$i\frac{\partial u}{\partial t}+\frac{1}{2}\frac{\partial^2 u}{\partial x^2}-V_2x^2u+|u|^2u=0, \tag{2.5}$$

where $V_2=\omega_x^2/(2\omega_\perp^2)$ is a small parameter characterizing the strength of the external parabolic potential. In the experiment of Rice University [17], a matter-wave soliton train (comprising $N\sim 10$ solitons) of Bose-condensed ^{7}Li atoms ($a_s=-0.21$ nm, $m=11.65\times10^{-27}$ kg) was created. Radial confinement was strong, $\omega_\perp\sim 800$ Hz, while the axial one had been as weak as $\omega_x\sim 3$ Hz. In the experiment [19], where a single soliton of ^{7}Li BEC was created, the trap aspect ratio was smaller: $\omega_\perp\sim 710$ Hz, $\omega_x\sim 50$ Hz. Therefore, $V_2\sim 10^{-5}-10^{-3}$ is in the range of realistic experimental conditions. Below we shall consider also other kinds of weak potentials in the axial direction x, instead of (or combined with) the parabolic trap in Eq. (2.5), see [20,21]. Assuming them as perturbations $iR[u]=V(x)u(x,t)$, we move them to the right hand side of the governing equation.

The N-soliton train interactions for the nonlinear Schrödinger equation (NLS) and its perturbed versions,

$$i\frac{\partial u}{\partial t}+\frac{1}{2}\frac{\partial^2 u}{\partial x^2}+|u|^2u=i\epsilon R[u], \tag{2.6}$$

started with the pioneering paper [22], and by now has been extensively studied (see [7–10,13] and references therein). Several other nonlinear evolution equations (NLEE) were also studied, among them the modified NLS equation [11,23,25–27], some higher NLS equations [13], the Ablowitz-Ladik system [24], and others.

Below we concentrate on the perturbed NLS Eq. (2.6). By "N-soliton train" we mean a solution of the (perturbed) NLS fixed up by the initial condition

$$u(x,t=0)=\sum_{k=1}^{N}u_{\mathrm{k}}^{1s}(x,t=0),\quad u_{\mathrm{k}}^{1s}(x,t)=\frac{2\nu_k e^{i\phi_k}}{\cosh z_k}, \tag{2.7}$$

$$z_k(x,t)=2\nu_k[x-\xi_k(t)],\quad \xi_k(t)=2\mu_k t+\xi_{k,0}, \tag{2.8}$$

$$\phi_k(x,t)=\frac{\mu_k}{\nu_k}z_k+\delta_k(t),\quad \delta_k(t)=W_k t+\delta_{k,0}, \tag{2.9}$$

Each soliton has four parameters: amplitude ν_k, velocity μ_k, center of mass position ξ_k, and phase δ_k. The adiabatic approximation uses as a small parameter $\varepsilon_0 \ll 1$ the soliton overlap which falls off exponentially with the distance between the solitons. Then the soliton parameters must satisfy [22]

$$|\nu_k-\nu_0|\ll\nu_0,\quad |\mu_k-\mu_0|\ll\mu_0,$$
$$|\nu_k-\nu_0||\xi_{k+1,0}-\xi_{k,0}|\gg 1, \tag{2.10}$$

where $\nu_0=\frac{1}{N}\sum_{k=1}^{N}\nu_k$ and $\mu_0=\frac{1}{N}\sum_{k=1}^{N}\mu_k$ are the average amplitude and velocity, respectively. In fact, we have two different scales,

$$|\nu_k-\nu_0|\simeq\varepsilon_0^{1/2},\quad |\mu_k-\mu_0|\simeq\varepsilon_0^{1/2},$$
$$|\xi_{k+1,0}-\xi_{k,0}|\simeq\varepsilon_0^{-1}.$$

One can expect that the approximation holds only for such times t for which the set of $4N$ parameters of the soliton train satisfy (2.10).

Equation (2.6) finds a number of applications to nonlinear optics and for $R[u]\equiv 0$ is integrable via the inverse scattering transform method [28,29]. The N-soliton train dynamics in the adiabatic approximation is modeled by a complex generalization of the Toda chain [7,8],

$$\frac{d^2Q_j}{dt^2}=16\nu_0^2(e^{Q_{j+1}-Q_j}-e^{Q_j-Q_{j-1}}),\quad j=1,\ldots,N. \tag{2.11}$$

The complex-valued Q_k are expressed through the soliton parameters by

$$Q_k(t)=2i\lambda_0\xi_k(t)+2k\ln(2\nu_0)+i[k\pi-\delta_k(t)-\delta_0], \tag{2.12}$$

where $\delta_0=1/N\sum_{k=1}^{N}\delta_k$ and $\lambda_0=\mu_0+i\nu_0$. Besides we assume free-ends conditions, i.e., $e^{-Q_0}\equiv e^{Q_{N+1}}\equiv 0$.

Note that the N-soliton train is *not* an N-soliton solution. The spectral data of the corresponding Lax operator L are nontrivial also on the continuous spectrum of L. Therefore, the analytical results from the soliton theory cannot be applied. Besides, we want to treat solitons moving with equal velocities and also to account for the effects of possible nonintegrable perturbations $R[u]$.

The fact [30,31] that the CTC, like the (real) Toda chain (RTC) [30], is a completely integrable Hamiltonian system allows one to analyze analytically the asymptotic behavior of the N-soliton trains. However, unlike the RTC, the CTC has a richer variety of dynamical regimes [7,10,32] such as (i) asymptotically free motion if $v_j\neq v_k$ for $j\neq k$; this is the only dynamical regime possible for RTC; (ii) N-s bound state if $v_1=\cdots=v_N$ but $\zeta_k\neq\zeta_j$ for $k\neq j$; (iii) various intermediate (mixed) regimes, e.g., if $v_1=v_2>\cdots>v_N$ but $\zeta_k\neq\zeta_j$, for $k\neq j$, then we will have a bound state of the first two solitons while all the others will be asymptotically free; (iv) singular and degenerate regimes if two or more of the eigenvalues of L become equal, e.g., $\zeta_1=\zeta_2\cdots$ and $\zeta_j\neq\zeta_k$ for $2<j\neq k$.

By $\zeta_k=v_k+iw_k$ above we have denoted the eigenvalues of the Lax matrix L in the Lax representation $L_\tau=[M,L]$ of the CTC, where

$$L=\sum_{k=1}^{N}b_kE_{kk}+\sum_{k=1}^{N-1}a_k(E_{k,k+1}+E_{k+1,k}), \tag{2.13}$$

where

$$b_k\equiv-\frac{1}{2}\frac{dQ_k}{d\tau}=\frac{\mu_k+i\nu_k}{2},\quad a_k=\frac{1}{2}e^{(Q_{k+1}-Q_k)/2},$$

and the matrices E_{kp} are defined by $(E_{kp})_{ij}=\delta_{ki}\delta_{pj}$. The eigenvalues ζ_k of L are time-independent and complex-valued along with the first components $\eta_k=\vec{z}_1^{(k)}$ of the normalized eigenvectors of L,

$$L\vec{z}^{(k)}=\zeta_k\vec{z}^{(k)},\quad (\vec{z}^{(k)},\vec{z}^{(m)})=\delta_{km}. \tag{2.14}$$

The set of $\{\zeta_k=v_k+iw_k,\ \eta_k=\sigma_k+i\theta_k\}$ may be viewed as the set of action-angle variables of the CTC.

Using the CTC model, one can determine the asymptotic regime of the N-soliton train. Given the initial parameters $\mu_k(0),\nu_k(0),\xi_k(0),\delta_k(0)$ of the N-soliton train, one can calculate the matrix elements b_k and a_k of L at $t=0$. Then solving the characteristic equation on $L|_{t=0}$ one can calculate the eigenvalues ζ_k to determine the asymptotic regime of the N-soliton train [7,10]. Another option is to impose on ζ_k a specific constraint, e.g., that all ζ_k be purely imaginary, i.e., all $v_k=0$. This will provide a set of algebraic conditions $L|_{t=0}$, and on the initial soliton parameters $\mu_k(0),\nu_k(0),\xi_k(0),\delta_k(0)$ which characterize the region in the soliton parameter space responsible for the N-soliton bound states.

III. THE PERTURBED NLS AND PERTURBED CTC EQUATIONS

We will consider several specific choices $R^{(p)}[u]$ of perturbations, $p=1,2,\ldots$, in Eq. (2.6). In the adiabatic approximation, the dynamics of the soliton parameters can be determined by the system (see [22] for $N=2$ and [7,10] for $N>2$)

$$\frac{d\lambda_k}{dt} = -4\nu_0(e^{Q_{k+1}-Q_k} - e^{Q_k-Q_{k-1}}) + M_k^{(p)} + iN_k^{(p)}, \quad (3.1)$$

$$\frac{d\xi_k}{dt} = 2\mu_k + \Xi_k^{(p)}, \quad \frac{d\delta_k}{dt} = 2(\mu_k^2+\nu_k^2) + X_k^{(p)}, \quad (3.2)$$

where $\lambda_k=\mu_k+i\nu_k$ and $X_k^{(p)}=2\mu_k\Xi_k^{(p)}+D_k^{(p)}$. The right hand sides of Eqs. (3.1) and (3.2) are determined by $R_k^{(p)}[u]$ through

$$N_k^{(p)} = \frac{1}{2}\int_{-\infty}^{\infty} \frac{dz_k}{\cosh z_k}\,\mathrm{Re}(R_k^{(p)}[u]e^{-i\phi_k}), \quad (3.3)$$

$$M_k^{(p)} = \frac{1}{2}\int_{-\infty}^{\infty} \frac{dz_k \sinh z_k}{\cosh^2 z_k}\,\mathrm{Im}(R_k^{(p)}[u]e^{-i\phi_k}), \quad (3.4)$$

$$\Xi_k^{(p)} = \frac{1}{4\nu_k^2}\int_{-\infty}^{\infty} \frac{dz_k z_k}{\cosh z_k}\,\mathrm{Re}(R_k^{(p)}[u]e^{-i\phi_k}), \quad (3.5)$$

$$D_k^{(p)} = \frac{1}{2\nu_k}\int_{-\infty}^{\infty} \frac{dz_k(1-z_k\tanh z_k)}{\cosh z_k}\,\mathrm{Im}(R_k^{(p)}[u]e^{-i\phi_k}). \quad (3.6)$$

Inserting Eqs. (3.1) and (3.2) into Eq. (2.12), we derive

$$\frac{dQ_k}{dt} = -4\nu_0\lambda_k + \frac{2k}{\nu_0}\mathcal{N}_0^{(p)} + 2i\xi_k(\mathcal{M}_0^{(p)} + i\mathcal{N}_0^{(p)}) + i(2\lambda_0\Xi_k^{(p)} - X_k^{(p)} - \mathcal{X}_0^{(p)}), \quad (3.7)$$

$$\mathcal{N}_0^{(p)} = \frac{1}{N}\sum_{j=1}^{N} N_j^{(p)}, \quad \mathcal{M}_0^{(p)} = \frac{1}{N}\sum_{j=1}^{N} M_j^{(p)},$$

$$\mathcal{X}_0^{(p)} = \frac{1}{N}\sum_{j=1}^{N} X_j^{(p)}.$$

In deriving Eq. (3.7) we have kept terms of the order $\Delta\nu_k \simeq O(\sqrt{\epsilon_0})$ and neglected terms of the order $O(\epsilon_0)$. The perturbations may result in ν_0 and μ_0 becoming time-dependent. Indeed, from Eq. (3.1) we get

$$\frac{d\mu_0}{dt} = \mathcal{M}_0^{(p)}, \quad \frac{d\nu_0}{dt} = \mathcal{N}_0^{(p)}. \quad (3.8)$$

The small parameter ϵ_0 can be related to the initial distance $r_0=|\xi_2-\xi_1|_{t=0}$ between the two solitons. Assuming $\nu_{1,2}\simeq\nu_0$, we find

$$\epsilon_0 = \int_{-\infty}^{\infty} dx|u_1^{1s}(x,0)u_2^{1s}(x,0)| \simeq 8\nu_0 r_0 e^{-2\nu_0 r_0}. \quad (3.9)$$

In particular, Eq. (3.9) means that $\epsilon_0\simeq 0.01$ for $r_0\simeq 8$ and $\nu_0=1/2$.

We assume that initially the solitons are ordered in such a way that $\xi_{k+1}-\xi_k\simeq r_0$. One can check [8,11] that $N_k^{(p)} \simeq M_k^{(p)} \simeq \exp(-2\nu_0|k-p|r_0)$. Therefore, the interaction terms between the kth and $(k\pm1)$st solitons will be of the order of $e^{-2\nu_0 r_0}$; the interactions between the kth and $(k\pm2)$nd soliton will of the order of $e^{-4\nu_0 r_0} \ll e^{-2\nu_0 r_0}$.

The terms $\Xi_k^{(0)}$, $X_k^{(0)}$ are of the order of $r_0^a\exp(-2\nu_0 r_0)$, where $a=0$ or 1. However, they can be neglected as compared to $\tilde{\mu}_k$ and $\tilde{\nu}_k$, where

$$\tilde{\mu}_k = \mu_k - \mu_0 \simeq \sqrt{\epsilon_0}, \quad \tilde{\nu}_k = \nu_k - \nu_0 \simeq \sqrt{\epsilon_0}. \quad (3.10)$$

The corrections to $N_k^{(p)}$, $p=1,2,\ldots$, coming from the terms linear in u depend only on the parameters of the kth soliton, i.e., they are "local" in k. The nonlinear terms in u present in $iR^{(p)}[u]$ produce also "nonlocal" in k terms in $N_k^{(p)}$, $p=1,2,\ldots$.

A. Quadratic and tilted potentials

Let $iR[u]=V(x)u(x,t)$. Our first choice for $V(x)$ is a quadratic one,

$$V^{(1)}(x) = V_2x^2 + V_1x + V_0. \quad (3.11)$$

From the above analysis, we get the results

$$N_k^{(1)} = 0, \quad \Xi_k^{(1)} = 0, \quad (3.12a)$$

$$M_k^{(1)} = -V_2\xi_k - \frac{V_1}{2}, \quad (3.12b)$$

$$D_k^{(1)} = V_2\left(\frac{\pi^2}{48\nu_k^2} - \xi_k^2\right) - V_1\xi_k - V_0, \quad (3.12c)$$

and $X_k^{(1)}=D_k^{(1)}$. As a result, the corresponding PCTC takes the form [13]

$$\frac{d\lambda_k}{dt} = -4\nu_0(e^{Q_{k+1}-Q_k} - e^{Q_k-Q_{k-1}}) - V_2\xi_k - \frac{V_1}{2}, \quad (3.13)$$

$$\frac{dQ_k}{dt} = -4\nu_0(\mu_k + i\nu_k) - iD_k^{(1)} - \frac{i}{N}\sum_{j=1}^{N} D_j^{(1)}, \quad (3.14)$$

where $\lambda_k=\mu_k+i\nu_k$.

If we now differentiate Eq. (3.14) and make use of Eq. (3.13), we get [13]

$$\frac{d^2Q_k}{dt^2} = 16\nu_0^2(e^{Q_{k+1}-Q_k} - e^{Q_k-Q_{k-1}}) + 4\nu_0\left(V_2\xi_k + \frac{V_1}{2}\right) - i\frac{dD_k^{(1)}}{dt} - \frac{i}{N}\sum_{j=1}^{N}\frac{dD_j^{(1)}}{dt}. \quad (3.15)$$

It is reasonable to assume that $V_2\simeq O(\epsilon_0/N)$; this ensures the possibility to have the N-soliton train "inside" the potential. It also means that both the exponential terms and the correction terms $M_k^{(1)}$ are of the same order of magnitude. From Eqs. (3.13) and (3.14) it follows that $d\nu_0/dt=0$ and

$$\frac{d\mu_0}{dt} = -V_2\xi_0 - \frac{V_1}{2}, \quad \frac{d\xi_0}{dt} = 2\mu_0, \tag{3.16}$$

where μ_0 is the average velocity and $\xi_0=\frac{1}{N}\sum_{j=1}^{N}\xi_j$ is the center of mass of the N-soliton train. The system of Eqs. (3.16) for $V_2>0$ has a simple solution

$$\mu_0(t) = \mu_{00}\cos[\Phi(t)],$$

$$\xi_0(t) = \sqrt{\frac{2}{V_2}}\mu_{00}\sin[\Phi(t)] - \frac{V_1}{2V_2}, \tag{3.17}$$

where $\Phi(t)=\sqrt{2V_2}t+\Phi_0$, and μ_{00} and Φ_0 are constants of integration. Therefore, the overall effect of such a quadratic potential will be to induce a slow periodic motion of the train as a whole.

By tilted potential below we mean a particular case of the quadratic potential with $V_2=0$. Then Eqs. (3.16) and (3.17) take the form

$$\frac{d\tilde{\mu}_0}{dt} = -\frac{V_1}{2}, \quad \frac{d\tilde{\xi}_0}{dt} = 2\tilde{\mu}_0, \tag{3.18}$$

and have the simple solution

$$\tilde{\mu}_0(t) = -\frac{V_1}{2}t + \tilde{\mu}_{00},$$

$$\tilde{\xi}_0(t) = -\frac{V_1}{4}t^2 + \tilde{\mu}_{00}t + \tilde{\xi}_{00}. \tag{3.19}$$

Therefore, the tilted potential accelerates the soliton train as a whole in a prescribed direction. It can be used also to "pick up" and accelerate one or more of the solitons from the train confined to a periodic potential.

B. Periodic potentials

One may consider several physically important choices of periodic potentials. The simplest one is

$$V^{(2)}(x) = A_1\cos(\Omega_1 x + \Omega_0) = A_1 - 2A_1\sin^2(\Omega_1 x/2 + \Omega_0/2), \tag{3.20}$$

where A, Ω, and Ω_0 are appropriately chosen constants. The NLS equation with similar potentials appears in a natural way in the study of Bose-Einstein condensates, see [20].

The relevant integrals for N_k, M_k, Ξ_k, and D_k are equal to [13]

$$N_k^{(2)} = 0, \quad \Xi_k^{(2)} = 0, \tag{3.21}$$

$$M_k^{(2)} = \frac{\pi A_1\Omega_1^2}{8\nu_k}\frac{1}{\sinh Z_k}\sin(\Omega_1\xi_k + \Omega_0), \tag{3.22}$$

$$D_k^{(2)} = -\frac{\pi^2 A_1\Omega_1^2}{16\nu_k^2}\frac{\cosh Z_k}{\sinh^2 Z_k}\cos(\Omega_1\xi_k + \Omega_0), \tag{3.23}$$

where $Z_{1,k}=\pi\Omega_1/(4\nu_k)$. These results allow one to derive the corresponding perturbed CTC models. Again we find that $d\nu_0/dt=0$.

The second case we will consider is a linear combination of two potentials of the form (3.20) with correlated frequencies,

$$V^{(3)}(x) = A_1\cos(\Omega_1 x + \Omega_0) + A_2\cos(\Omega_2 x + \Omega_0), \tag{3.24}$$

where A_j, Ω_j, and Ω_0 are appropriately chosen constants. Such potentials with rationally related frequencies, e.g., $\Omega_2=2\Omega_1$, also appear in the study of Bose-Einstein condensates, see [20].

The relevant integrals for N_k, M_k, Ξ_k, and D_k are equal to [13]

$$N_k^{(3)} = 0, \quad \Xi_k^{(3)} = 0, \tag{3.25}$$

$$\begin{aligned} M_k^{(3)} &= A_1 M_k(\Omega_1, Z_{1,k})\sin(\Omega_1\xi_k + \Omega_0) \\ &\quad + A_2 M_k(\Omega_2, Z_{2,k})\sin(\Omega_2\xi_k + \Omega_0), \end{aligned} \tag{3.26}$$

$$\begin{aligned} D_k^{(3)} &= A_1 D_k(\Omega_1, Z_{1,k})\cos(\Omega_1\xi_k + \Omega_0) \\ &\quad + A_2 D_k(\Omega_2, Z_{2,k})\cos(\Omega_2\xi_k + \Omega_0), \end{aligned} \tag{3.27}$$

where

$$M_k(\Omega_j, Z_{j,k}) = \frac{\pi\Omega_j^2}{8\nu_k}\frac{1}{\sinh Z_{j,k}},$$

$$D_k(\Omega_j, Z_{j,k}) = -\frac{\pi^2\Omega_j^2}{16\nu_k^2}\frac{\cosh Z_{j,k}}{\sinh^2 Z_{j,k}}, \tag{3.28}$$

$Z_{j,k}=\pi\Omega_j/(4\nu_k)$. These results allow one to derive the corresponding perturbed CTC models. Again we find that $d\nu_0/dt=0$.

The last case we consider is an elliptic potential of the form

$$V^{(4)}(x) = -B\,\mathrm{sn}^2(\Omega x; k) = -B\sum_{s=0}^{\infty} G_s(k)\sin(\Omega_s x), \tag{3.29}$$

$$G_s(k) = \left(\frac{1+k^2}{2k^3} - \frac{(2s+1)^2\pi^2}{8k^3K^2}\right)\frac{\pi}{K\sinh(\omega_s)}, \tag{3.30}$$

$$\Omega_s = \frac{(2s+1)\pi}{2K}\Omega, \quad \omega_s = \frac{(2s+1)\pi K'}{2K}, \tag{3.31}$$

where k is the module of the elliptic function, $K=K(k)$ is the complete elliptic integral of the first kind, and B is a constant.

The second line of formula (3.29) provides the expansion of $\mathrm{sn}^2(\Omega x; k)$ as infinite series of trigonometric functions. Each of the terms in this series can be treated as a perturbation just like above assuming $\Omega_0=-\pi/2$. As a result, we get

$$N_k^{(4)} = 0, \quad \Xi_k^{(4)} = 0, \tag{3.32}$$

$$M_k^{(4)} = B\sum_{s=0}^{\infty} M_k(\Omega_s, Z_{s,k})G_s(k)\cos(\Omega_s\xi_k), \tag{3.33}$$

$$D_k^{(4)} = -B\sum_{s=0}^{\infty} D_k(\Omega_s, Z_{s,k})G_s(k)\sin(\Omega_s\xi_k), \qquad (3.34)$$

where M_k, D_k, and $\Omega_s=(2s+1)\Omega$ are defined as in Eq. (3.28).

IV. CTC ANALYSIS AND COMPARISON WITH NUMERICAL SIMULATIONS

The dynamics of an individual soliton in a train is determined by the combined action of external potential and the influence of neighboring solitons. The interaction with neighboring solitons can be either repulsive or attractive, depending on the phase relations between them. Particularly, if their amplitudes are equal and the initial phase difference between neighboring solitons is π (as considered below), they repel each other giving rise to expanding motion in the absence of an external field [7,8].

The external potential counterbalances the expansion, trying to confine solitons in the minima of the potential. It is the interplay of these two factors, the interaction of solitons and the action of the external potential, which gives rise to a rich dynamics of the N-soliton train.

To verify the adequacy of the perturbed CTC model for the description of the N-soliton train dynamics in external potentials, we performed a comparison of predictions of the corresponding perturbed CTC (PCTC) system and direct simulations of the underlying NLS equation (2.6). Below we present results pertaining to a matter-wave soliton train in a confining (i) parabolic trap and (ii) a periodic potential modeling an optical lattice.

Here we present the numerical verification of the PCTC model. The perturbed NLS Eq. (2.6) is solved by the operator splitting procedure using the fast Fourier transform [33]. In the course of time, we monitor the conservation of the norm and energy of the N-soliton train. The corresponding PCTC equations are solved by the Runge-Kutta scheme with the adaptive step-size control [34].

The evolution of an N-soliton train in the absence of potential $[V(x)=0]$ is well known; see, e.g., [8,10]. These papers propose a method to determine the asymptotic dynamical regime of the CTC for a given set of initial parameters $\nu_k(0)$, $\mu_k(0)$, $\xi_k(0)$, and $\delta_k(0)$. Below we will use mainly the following set of parameters: $\nu_k(0)=1/2$, $\mu_k(0)=0$, $\xi_{k+1}(0)-\xi_k(0)=r_0$, with two different choices for the phases,

$$\delta_k(0) = k\pi, \qquad (4.1)$$

$$\delta_k(0) = 0. \qquad (4.2)$$

These two types of initial conditions (IC) are most widely used in numeric simulations.

In the absence of potential, the IC (4.1) ensure the so called free asymptotic regime, i.e., each soliton develops its own velocity and the distance between the neighboring solitons increases linearly in time. At the same time, the center of mass of the soliton train stays at rest (see the upper panel of Fig. 1). Under the IC (4.2), the solitons attract each other going into collisions whenever the distance between them is not large enough.

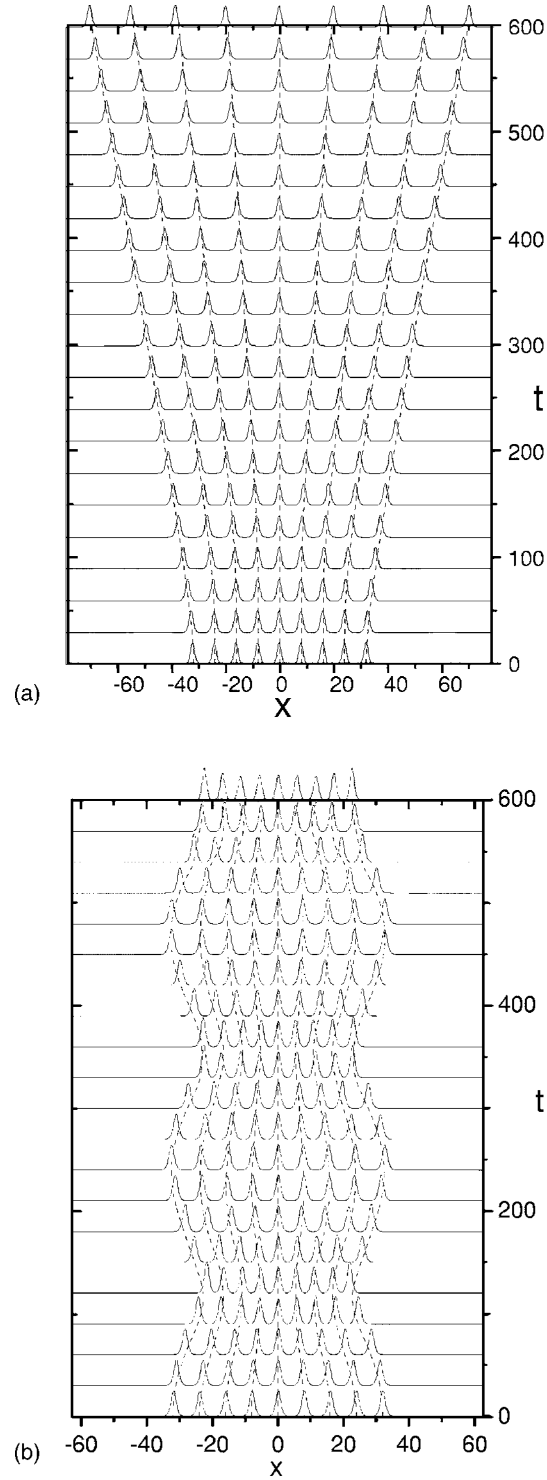

FIG. 1. Upper panel: nine-soliton train with initial parameters as in Eq. (4.1) with $r_0=8$ in the absence of a potential goes into the free asymptotic regime. Solid lines: direct numerical simulation of the NLS equation (2.6); dashed lines: $\xi_k(t)$ as predicted by the CTC equations (4.3)–(4.6) with $V_0=V_1=V_2=0$ and $r_0=8$. Lower panel: Evolution of a nine-soliton train with the same initial parameters in the quadratic potential $V(x)=V_2x^2$ with $V_2=0.00005$. Solid lines: direct numerical simulation of the NLS equation (2.6); dashed lines: solution of the PCTC equations (4.3)–(4.6). Initially the train is placed symmetrically relative to the minimum of the potential at $x=0$.

From a mathematical point of view, the IC (4.1) reduce the CTC into a standard (real) Toda chain for which the free asymptotic regime is the only possible asymptotical regime. On the contrary, the IC (4.2) lead to singular solutions for the CTC (see [7,10,32]). The singularities of the exact solutions for the CTC coincide with the positions of the collisions.

Below we will study the effects of the potentials for both types of IC. One may expect that the quadratic potential will prevent a free asymptotic regime of IC (4.1) no matter how small $V_2>0$ is and would not be able to prevent collisions in the case of IC (4.2). The periodic potential, if strong enough, should be able to stabilize and bring to bound states both types of IC.

A. Quadratic potential

For the quadratic external potential $V(x)=V_2x^2+V_1x+V_0$, the perturbed CTC equations in terms of soliton parameters have the form

$$\frac{d\mu_k}{dt} = 16\nu_0^3(e^{-2\nu_0(\xi_{k+1}-\xi_k)}\cos\Phi_k - e^{-2\nu_0(\xi_k-\xi_{k-1})}\cos\Phi_{k-1}) - V_2\xi_k - \frac{V_1}{2}, \tag{4.3}$$

$$\frac{d\nu_k}{dt} = 16\nu_0^3(e^{-2\nu_0(\xi_{k+1}-\xi_k)}\sin\Phi_k - e^{-2\nu_0(\xi_k-\xi_{k-1})}\sin\Phi_{k-1}), \tag{4.4}$$

$$\frac{d\xi_k}{dt} = 2\mu_k, \tag{4.5}$$

$$\frac{d\delta_k}{dt} = 2(\mu_k^2+\nu_k^2) + V_2\left(\frac{\pi^2}{48\nu_k^2} - \xi_k^2\right) - V_1\xi_k - V_0, \tag{4.6}$$

$$\Phi_k = 2\mu_0(\xi_{k+1}-\xi_k) + \delta_k - \delta_{k+1}, \tag{4.7}$$

where μ_k, ν_k, ξ_k and δ_k for $k=1,\ldots,N$ are the $4N$ soliton parameters; see Eqs. (2.7) and (2.8).

The effect of the quadratic potential on the N-soliton train with parameters (4.1) is to balance the repulsive interaction between the solitons, so that they remain bounded by the potential, as illustrated in the lower panels of Figs. 1 and 2. The quadratic potentials are supposed to be weak, i.e., we choose V_2 so that

$$V_2\xi_N^2(0) \leqslant \nu_0, \quad V_2\xi_1^2(0) \leqslant \nu_0. \tag{4.8}$$

Figures 1 and 2 show good agreement between the PCTC model and the numerical solution of the perturbed NLS equation (2.6). They also show two types of effects of the quadratic potential on the motion of the N-soliton train: (i) the train performs contracting and expanding oscillations if its center of mass coincides with the minimum of the potential, (ii) the train oscillates around the minimum of the potential as a whole if its center of mass is shifted. In the last case, contracting and expanding motions of the soliton train is superimposed to the center of mass dynamics. As one can see from the figures, the period of this motion matches very well the one predicted by formula (3.17). Indeed, from Eq. (3.17) it follows that the period of the center of mass motion is $T=2\pi/\sqrt{2V_2}$. For the parameters in Fig. 2 we have $T\simeq 628$ (for a nine-soliton train), $T\simeq 140$ (for a three-soliton train). The dynamics are similar for the seven-soliton train in Fig. 3; for the parameters chosen there, we have $T\simeq 314$, in good agreement with the numerical simulations. The direct simulations of the NLS equation (2.6) show that a stronger parabolic trap may cause merging of individual solitons at

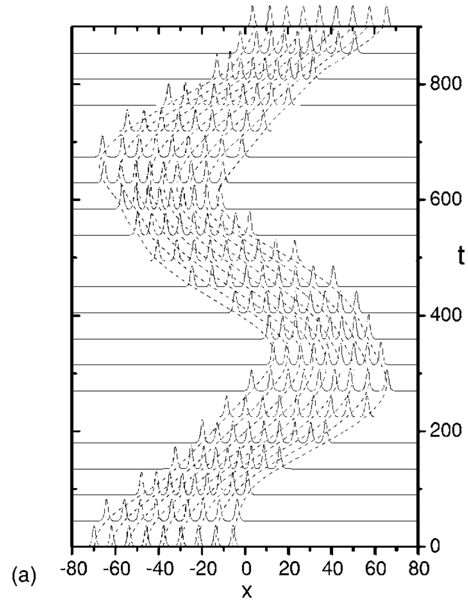

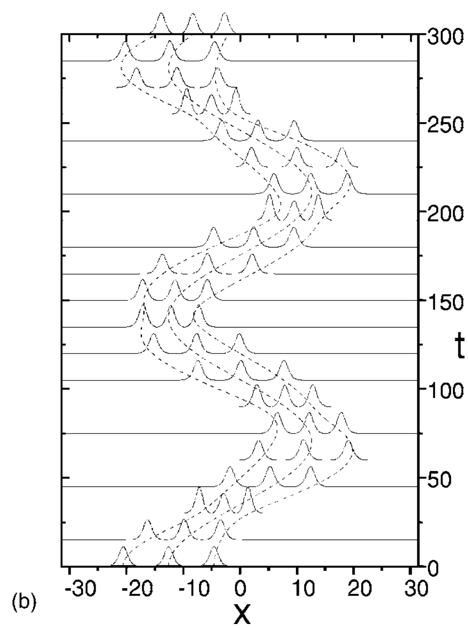

FIG. 2. Harmonic oscillations of an N-soliton train initially shifted relative to the minimum of the quadratic potential $V(x)=V_2x^2$. Upper panel: nine-soliton train, $V_2=0.00005$. Lower panel: three-soliton train, $V_2=0.001$. The IC of both trains is given by Eq. (4.1) with $r_0=8$. In both panels, solid lines correspond to direct simulations of the NLS equation (2.6), and dashed lines to numerical solution of the PCTC equations (4.3)–(4.6).

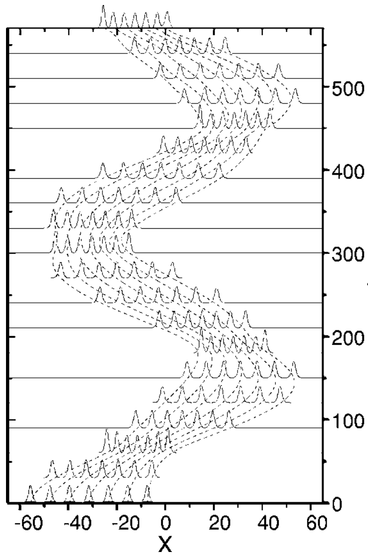

FIG. 3. Dynamics of a seven-soliton train placed asymmetrically relative to the minimum of the trap $V(x)=0.0002x^2$. Solid lines: results of direct numerical simulations of the NLS equation (2.6). Dashed lines: result of solution of the PCTC system (4.3)–(4.6) for the center of mass ξ_i. The parameters of solitons are the same as in Eq. (4.1) with $r_0=8$. The initial shift of the soliton train relative to the minimum of the parabolic trap is 10π.

times of contraction, and restoring of the original configuration when the train is expanded. This behavior is reminiscent of the phenomenon of "missing solitons" observed in the experiment [17]. However, this situation is beyond the validity of the PCTC approach.

B. Tilted periodic potential

Now we consider the dynamics of an N-soliton train in a tilted periodic potential, which is the combination of periodic and linear potentials,

$$V(x) = A\cos(\Omega x + \Omega_0) + Bx. \tag{4.9}$$

This potential is of particular interest in studies of Bloch oscillations of Bose-Einstein condensates. A train of repulsive BEC loaded in such a potential (where the periodic potential was a 1D optical lattice and the linear one was due to the gravitation) exhibits, indeed, Bloch oscillations [35]. At each period of these oscillations, condensate atoms residing in individual optical lattice cells coherently tunneled through the potential barriers. This was the first experimental demonstration of a pulsed atomic laser [35]. Recently, a new model of a pulsed atomic laser was theoretically developed in [36], where the solitons of attractive BEC were considered as carriers of coherent atomic pulses.

Controlled manipulation with matter-wave solitons is an important issue in these applications. Below we demonstrate that solitons of attractive BEC confined in an optical lattice can be flexibly manipulated by adjustment of the strength of the linear potential. In Fig. 4, we show the extraction of a different number of solitons from the five-soliton train by increasing the strength of the linear potential B, as obtained from direct simulations of the NLS equation (1) and numerical integration of the PCTC system (38)-(41) with

$$M_k^{(2)} = \frac{\pi A\Omega^2}{8\nu_k}\frac{1}{\sinh Z_k}\sin(\Omega\xi_k + \Omega_0) - \frac{1}{2}B, \tag{4.10}$$

$$D_k^{(2)} = -\frac{\pi^2 A\Omega^2}{16\nu_k^2}\frac{\cosh Z_k}{\sinh^2 Z_k}\cos(\Omega\xi_k + \Omega_0) - B\xi_k. \tag{4.11}$$

As is evident from Fig. 4, the PCTC model provides an adequate description of the dynamics of an N-soliton train in a tilted periodic potential. A small divergence between predictions for the trajectory of the left border soliton in Fig. 4(d) is due to the imperfect absorption of solitons from the right end of the integration domain. Reflected waves enter the integration domain and interact with solitons, which causes the discrepancy.

C. Periodic potential

Another external potential in which the N-soliton train exhibits interesting dynamics is the periodic potential of the form $V(x)=A\cos(\Omega x+\Omega_0)$. This case also may have a direct relevance to matter-wave soliton trains confined to optical lattices. The PCTC system in terms of soliton parameters has the form

$$\frac{d\mu_k}{dt} = 16\nu_0^3\left(e^{-2\nu_0(\xi_{k+1}-\xi_k)}\cos\Phi_k - e^{-2\nu_0(\xi_k-\xi_{k-1})}\cos\Phi_{k-1}\right) + M_k^{(2)}(\nu_k), \tag{4.12}$$

$$\frac{d\nu_k}{dt} = 16\nu_0^3\left(e^{-2\nu_0(\xi_{k+1}-\xi_k)}\sin\Phi_k - e^{-2\nu_0(\xi_k-\xi_{k-1})}\sin\Phi_{k-1}\right), \tag{4.13}$$

$$\frac{d\xi_k}{dt} = 2\mu_k, \tag{4.14}$$

$$\frac{d\delta_k}{dt} = 2(\mu_k^2 + \nu_k^2) + D_k^{(2)}(\nu_k), \tag{4.15}$$

where $M_k^{(2)}(\nu_k)$, $D_k^{(2)}(\nu_k)$ are given in Eqs. (3.21) and (3.23), and Φ_k in Eq. (4.7).

Each soliton of the train experiences the confining force of the periodic potential and the repulsive force of neighboring solitons. Therefore, equilibrium positions of solitons do not coincide with the minima of the periodic potential. Solitons placed initially at minima of the periodic potential (Fig. 5) perform small amplitude oscillations around these minima, provided that the strength of the potential is big enough to keep solitons confined. In contrast, the weak periodic potential is unable to confine solitons, and repulsive forces between neighboring solitons (at phase difference π) induces unbounded expansion of the train. In the intermediate region, when the confining force of the periodic potential is comparable with the repulsive forces of neighboring solitons, interesting dynamics can be observed such as the ex-

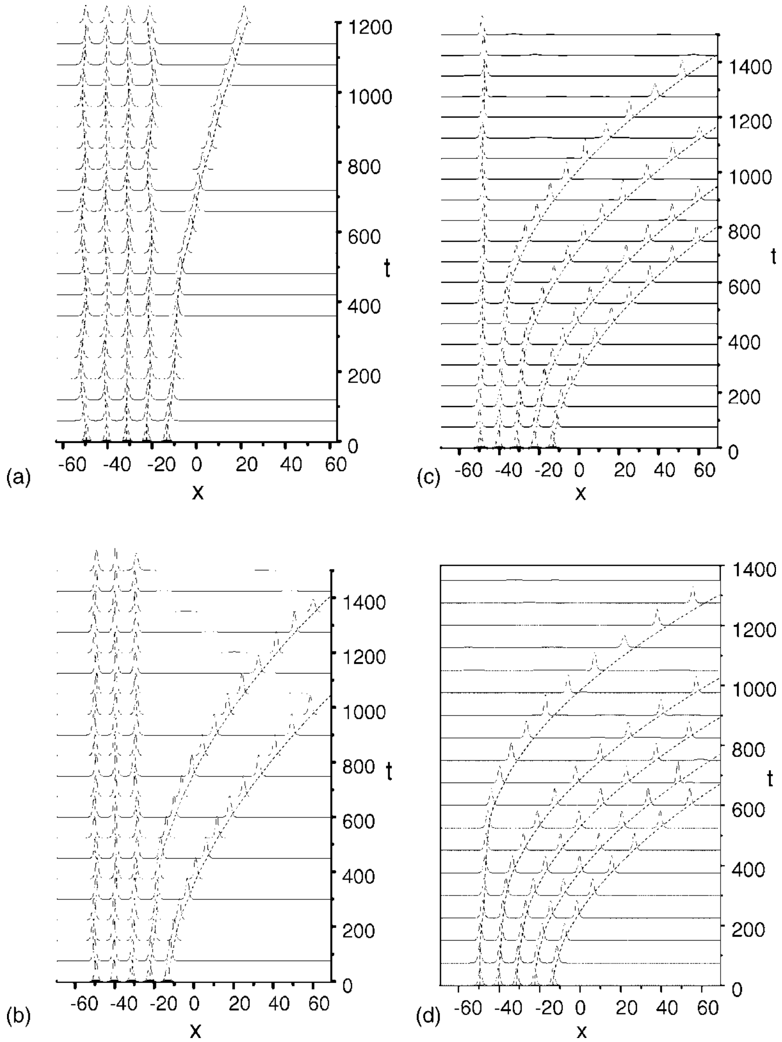

FIG. 4. Controlled withdrawal of solitons from the five-soliton train by adjusting the strength of the linear potential (4.9) with parameters: $A=-0.0005$, $\Omega=2\pi/9$, $\Omega_0=0$. Depending on the tilt, a different number of solitons can be pulled out of the train: (a) one soliton at $B=-0.00003$, (b) two at $B=-0.00011$, (c) four at $B=-0.0002$, and (d) five at $B=-0.0003$. The initial phase difference and separation between neighboring solitons in the train are, respectively, π and 9. Initially the train is shifted by -10π with respect to $x=0$ for graphical convenience. Solid and dashed lines correspond, respectively, to direct simulations of the NLS equation (2.6) and numerical integration of the PCTC system (4.12)–(4.15).

pulsion of bordering solitons from the train, as shown in the upper panel of Fig. 6. This phenomenon, revealing the complexity of the internal dynamics of the train, can be explained as follows. Each soliton performs nonlinear oscillations within individual potential wells under repulsive forces from neighboring solitons. When the amplitude of oscillations of particular solitons grows and two solitons closely approach each other, a strong recoil momentum can cause the soliton to leave the train, overcoming barriers of the periodic potential. In Fig. 6, this happens with bordering solitons (the other solitons remain bounded under long time evolution). It is noteworthy to stress that this phenomenon is well described by the PCTC model, as is evident from Fig. 6, upper panel.

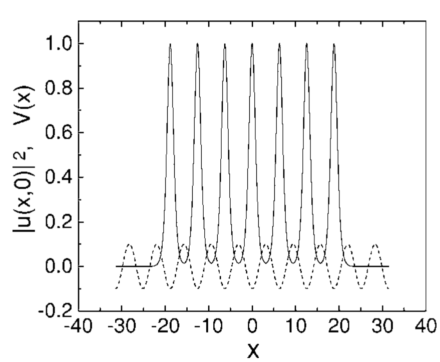

FIG. 5. Solitons (continuous line) remain confined around the minima of the periodic potential $V(x)=A\cos(x)$ (dashed line) performing small amplitude oscillations if its strength is big enough, $A=-0.1$.

On the lower panel of the same figure, we have similar IC as in Eq. (4.1) and we have chosen again the initial positions of the solitons to coincide with the minima of the periodic potential $V(x)=A\cos(\Omega x+\Omega_0)$, i.e., $r_0=2\pi/\Omega$. The values of $A=-0.0005$ and $r_0=9$ in the right panel of Fig. 6 now are such that the solitons form a bound state. Therefore, for any given initial distance r_0 there is a critical value $A_{\rm cr}(r_0)$ for A such that for $A>A_{\rm cr}(r_0)$ the soliton train with IC (4.1) will form a bound state.

In contrast to the quadratic potentials, the weak periodic potential is unable to confine solitons, and repulsive forces between neighboring solitons [at $\nu_k(0)=1/2$, $\delta_k(0)=k\pi$] induce unbounded expansion of the train similar to what was shown in the upper panel of Fig. 1.

The periodic potential can play a stabilizing role also for the IC (4.2), when the zero phase difference between neighboring solitons corresponds to their mutual attraction. If the periodic potential is strong enough, solitons do not experi-

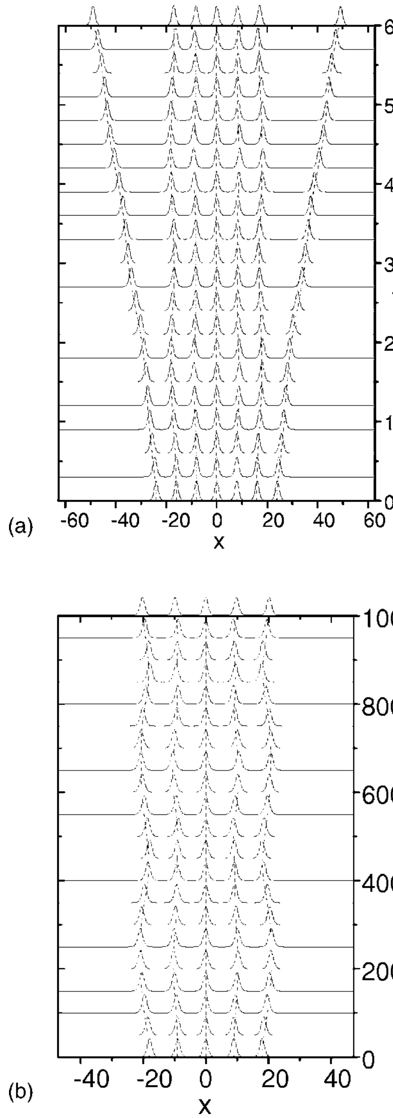

FIG. 6. Upper panel: The expulsion of solitons from the train, as obtained from direct simulations of the NLS equation (2.6) (solid lines), and as predicted by PCTC system (4.12)–(4.15) for the center of mass ξ_i (dashed lines). The IC of the seven-soliton train are given by Eq. (4.1) with $r_0=8$; the parameters of the periodic potential $V(x)=A\cos(\Omega x+\Omega_0)$ are $A=-0.001$, $\Omega=\pi/4$, $\Omega_0=0$. Lower panel: Oscillations of the five-soliton train with IC given by Eq. (4.1) with $r_0=9$; in a moderately weak periodic potential, $A=-0.0005$, $\Omega=2\pi/9$, $\Omega_0=0$. Solid and dashed lines correspond, respectively, to numerical solution of the NLS Eq. (2.6) and PCTC system (4.12)–(4.15).

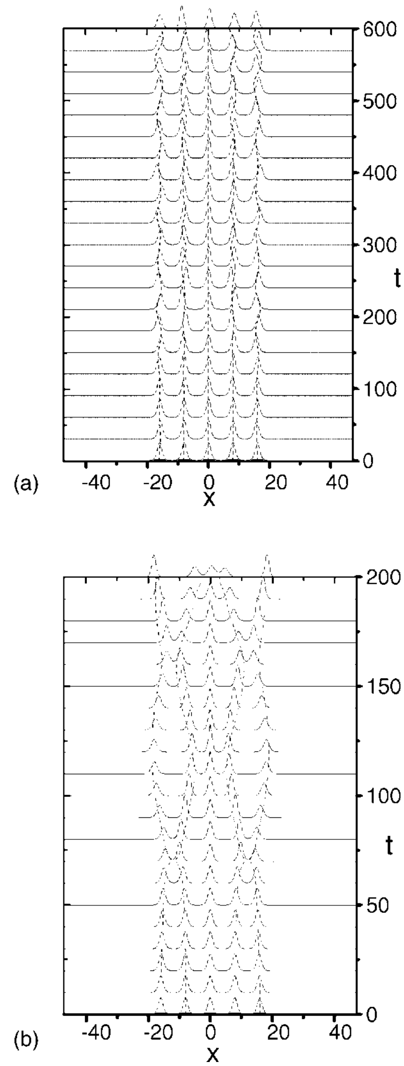

FIG. 7. Dynamics of a five-soliton train with zero phase difference between neighboring solitons, in the periodic potential $V(x)=A\cos(\Omega x+\Omega_0)$ with $\Omega=\pi/4$, $\Omega_0=0$, and $r_0=8$. Upper panel: When the periodic potential is strong enough $A=-0.02$, the N-soliton train remain confined, each soliton performing small amplitude oscillations around the minima of individual cells. Lower panel: Weaker periodic potential $A=-0.01$ cannot prevent solitons from collisions, which destroy the train. Solid and dashed lines correspond, respectively, to numerical solution of the NLS Eq. (2.6) and PCTC system (4.12)–(4.15).

ence collision. The weak periodic potential cannot prevent solitons from collisions, which eventually leads to destruction of the soliton train, as illustrated in Fig. 7. Again for any given initial distance r_0 there will be a critical value $A'_{\mathrm{cr}}(r_0)$ for A such that for $A>A'_{\mathrm{cr}}(r_0)$ the soliton train with IC (4.2) will form a bound state avoiding collisions.

Attractive interactions at zero phase difference between neighboring solitons can be balanced by expulsive force on solitons, if the train is positioned on an inverted parabolic trap. In this case, solitons far from the center experience stronger expulsive force and leave the train, as illustrated in Fig. 8.

V. HAMILTONIAN APPROACH TO PERTURBED NLS AND CTC

The Hamiltonian method has played an important role in the analysis of integrable and close to integrable nonlinear evolution equations and dynamical systems; see [29]. In this section, we will outline how this method can be used for the analysis of the N-soliton interactions.

The relation between the Hamiltonian properties of the NLS equation and the CTC model was derived in [37]. Here

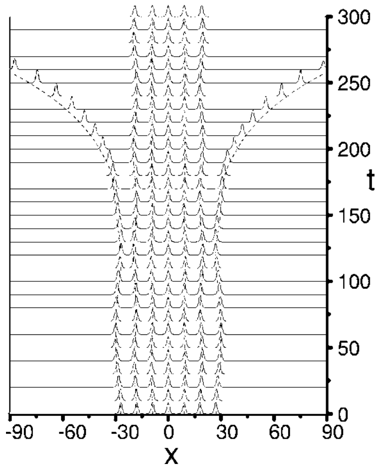

FIG. 8. Stabilization of a soliton train in a combined potential (periodic+inverted parabola): $V(x)=-0.02\cos(\Omega x)-0.000145x^2$. Separation between in-phase ($\delta_k=0$) solitons is $r_0=9$, $\Omega=2\pi/9$. Bordering solitons leave the train as they experience stronger expulsion, while the central ones remain bounded.

we will show that this approach can be extended also to the perturbed versions of NLS and CTC. Indeed, the Hamiltonian of Eq. (2.6) with $iR[u]=V(x)u(x,t)$ is equal to

$$H = H_{\rm NLS} + H_{\rm V}, \tag{5.1}$$

$$H_{\rm NLS} = \int_{-\infty}^{\infty} dx \frac{1}{2}[|u_x|^2 - |u(x,t)|^4], \tag{5.2}$$

$$H_{\rm V} = \int_{-\infty}^{\infty} dx V(x)|u(x,t)|^2. \tag{5.3}$$

One of the ways to derive the CTC from the NLS is based on the use of the variational method [9,38]. Namely, one constructs the Lagrangian of NLS, then takes an anzatz of the form

$$u(x,t) = \sum_{k=1}^{N} u_k^{(1s)}(x,t), \tag{5.4}$$

and integrates over x neglecting terms of order ϵ^k with $k>1$. Here $u_k^{(1s)}(x,t)$ is the one-soliton pulse with parameters μ_k, ν_k, ξ_k, and δ_k. The results must depend only on the $4N$-soliton parameters. It was pointed out in [37] that if we apply this method directly to the Hamiltonian $H_{\rm NLS}$, we get additional singular in ϵ elements which are taken care of by a proper regularization. The regularized Hamiltonian is

$$H_{\rm reg} = 4(\mu_0^2 + \nu_0^2)C_1 - 4\mu_0 C_2 + H_{\rm NLS},$$

$$C_1 = \int_{-\infty}^{\infty} dx|u(x,t)|^2,$$

$$C_2 = \int_{-\infty}^{\infty} dx \frac{i}{2}[u_x^* u(x,t) - u^*(x,t)u_x]. \tag{5.5}$$

Then one can show that

$$H_{\rm reg} = 32\nu_0 H_{\rm CTC} + \text{const}, \tag{5.6}$$

where $H_{\rm CTC}$ is the Hamiltonian of the CTC. It is obtained from the Toda chain Hamiltonian,

$$H_{\rm TC} = \sum_{k=1}^{N} \frac{1}{2}p_k^2 + \sum_{k=1}^{N-1} e^{q_{k+1}-q_k}, \tag{5.7}$$

by a complexification procedure after which the dynamical variables become complex-valued,

$$p_k \to P_k = p_{0,k} + ip_{1,k}, \quad q_k \to Q_k = q_{0,k} + iq_{1,k}, \tag{5.8}$$

which must satisfy the Poisson brackets,

$$\{p_{0,k}, q_{0,s}\} = \delta_{ks}, \quad \{p_{1,k}, q_{1,s}\} = -\delta_{ks}, \tag{5.9}$$

$$\{p_{0,k}, q_{1,s}\} = 0, \quad \{p_{1,k}, q_{0,s}\} = 0. \tag{5.10}$$

Then the CTC can be written down as a standard Hamiltonian system with $2N$ degrees of freedom and Hamiltonian provided by the real part of the complexified $H_{\rm TC}$,

$$H_{\rm CTC} = \sum_{k=1}^{N} \frac{1}{2}(p_{0,k}^2 - p_{1,k}^2) + 16\nu_0^2 \sum_{k=1}^{N-1} e^{q_{0,k+1}-q_{0,k}} \times\cos(q_{1,k+1} - q_{1,k}), \tag{5.11}$$

$$p_{0,k} = \frac{dq_{0,k}}{dt} = -4\nu_0\mu_k, \quad p_{1,k} = \frac{dq_{1,k}}{dt} = -4\nu_0\nu_k. \tag{5.12}$$

It remains to replace $q_{0,k}$ and $q_{1,k}$ in terms of the soliton parameters in order to get the final expression for $H_{\rm CTC}$.

Let us now derive the Hamiltonian for the perturbed CTC. To this end we will evaluate $H_{\rm V}$ in terms of the soliton parameters. Inserting the anzatz (5.4) into the integrand for $H_{\rm V}$ we obtain two types of terms. The first type is

$$H_{\rm V} = \sum_{k=1}^{N} H_k + \sum_{k=1}^{N} (H_{k,k-1} + H_{k,k+1}), \tag{5.13}$$

$$H_k = \int_{-\infty}^{\infty} dx V(x)|u_k^{(1s)}(x,t)|^2, \tag{5.14}$$

$$H_{k,k-1} = \int_{-\infty}^{\infty} dx V(x)(u_k^{(1s),*} u_{k-1}^{(1s)})(x,t).$$

In what follows, we will neglect the terms $H_{k,k-1}$ as compared to H_k, because their ratio is of the order of ϵ. The integrals in Eq. (5.14) for the quadratic and periodic potentials have the form

$$H_k = 4\nu_k\left[\left(V_2\xi_k^2 - \frac{\pi^2}{48\nu_k^2}\right) + V_1\xi_k + V_0\right] + \frac{\pi A\Omega}{\sinh Z_k}\cos(\Omega\xi_k + \Omega_0). \tag{5.15}$$

One can also evaluate the Poisson brackets between the soliton parameters inserting the expressions for $p_{\alpha,k}$ and $q_{\beta,s}$

with $\alpha,\beta=0,1$ into Eq. (5.9). We skip the lengthy calculations here and only note that these Poisson brackets combined with the Hamiltonian

$$H_{\mathrm{PCTC}} = H_{\mathrm{CTC}} + \sum_{k=1}^{N} H_k \tag{5.16}$$

$$= H_{\mathrm{CM}} + H_{\mathrm{V}}, \tag{5.17}$$

indeed produce the equations of motion for the PCTC.

Our next step is to separate the center of mass motion described by H_{CM},

$$H_{\mathrm{CM}} = N\left(8\nu_0^2(\mu_0^2-\nu_0^2) + 4\nu_0(V_2\xi_0^2 + V_1\xi_0 + V_0) - \frac{\pi A\Omega}{\sinh\left(\frac{\pi\Omega}{4\nu_0}\right)}\cos(\Omega\xi_0+\Omega_0)\right), \tag{5.18}$$

where the subscript 0 stands for the average value of the corresponding parameter, e.g., $\xi_0=1/N\Sigma_{k=1}^{N}\xi_k$. Then the Hamiltonian H_{V} would describe the relative motion of the solitons. We will express it as a function of the averaged parameters $\mu_0,\ldots,\delta_0$ and the relative parameters,

$$\tilde{\mu}_k = \mu_k - \mu_0, \quad \tilde{\nu}_k = \nu_k - \nu_0,$$

$$\tilde{\xi}_k = \xi_k - \xi_0, \quad \tilde{\delta} = \delta_k - \delta_0. \tag{5.19}$$

Note that only $N-1$ of the relative parameters are independent; obviously they satisfy $\Sigma_{k=1}^{N}\tilde{X}_k=0$, where $\tilde{X}_k$ stands for $\tilde{\mu}_k,\ldots,\tilde{\delta}_k$.

In evaluating H_{V} we will neglect higher-order terms, i.e., terms of the order $\epsilon^{3/2}$ and higher, as well as terms of the order $V_s\epsilon^{1/2}$, $A\epsilon^{1/2}$, and higher. As a result, H_{CM} and H_{V} simplify to

$$H_{\mathrm{CM}} = 8\nu_0^2(\mu_0^2-\nu_0^2) + 4\nu_0\left(V_2\xi_0^2 + V_1\xi_0 + V_0 - \frac{V_2\pi^2}{48\nu_0^2}\right) + \frac{\pi A\Omega}{\sinh Z_0}\cos(\Omega\xi_0+\Omega_0), \tag{5.20}$$

$$H_{\mathrm{V}} = 8\nu_0^2\sum_{k=1}^{N}(\tilde{\mu}_k^2 - \tilde{\nu}_k^2 + \tilde{H}_k) + 16\nu_0^2\sum_{k=1}^{N-1} e^{q_{0,k+1}-q_{0,k}}\cos(q_{1,k+1} - q_{1,k}), \tag{5.21}$$

$$\tilde{H}_k = 4\nu_0V_2(\xi_k-\xi_0)^2 + \frac{\pi A\Omega}{\sinh Z_0}[\cos(\Omega\xi_k+\Omega_0) - \cos(\Omega\xi_0+\Omega_0)]. \tag{5.22}$$

The Hamiltonian H_{CM} which describes the center of mass motion is more simple than H_{V} and often one is able to solve explicitly the corresponding equations of motion, see Sec. IV. The next step would be, using the known expressions for the averaged variables $\mu_0(t),\ldots,\delta_0(t)$, to insert them into H_{V} and try to analyze the corresponding equations of motion. This would provide us with information about the relative motion of the solitons around the center of mass. Usually we get a set of nonlinear and nonintegrable ODE.

TABLE I. The values of $A_{\mathrm{cr}}^{\mathrm{exp}}$ obtained from numeric simulations with PCTC versus $A_{\mathrm{cr}}^{\mathrm{th}}$ obtained from Eq. (5.23) for $N=3$.

r_0	$A_{\mathrm{cr}}^{\mathrm{exp}}$	$A_{\mathrm{cr}}^{\mathrm{th}}$	$A_{\mathrm{cr}}^{\mathrm{exp}}/A_{\mathrm{cr}}^{\mathrm{th}}$
2π	−0.0053	−0.00365	1.45
7	−0.0025	−0.00166	1.51
8	−0.00084	−0.00057	1.47
9	−0.00030	−0.00020	1.50

Our idea here is to use the explicit form of H_{V} for the estimation of the critical values of potential strengths A, V_2, V_1 for which the soliton motion becomes qualitatively different. Doing this we are making use of the following hypothesis based on the well known fact that bound states have negative energies while asymptotically free motions should correspond to positive energies. Therefore, we evaluate the Hamiltonian H_{V} inserting in it the initial soliton parameters along with the known expressions for $\mu_0,\ldots,\delta_0$. If the result is negative, we may expect that the relative motion of the solitons will be bounded; otherwise one may expect that at least one (or more) of the solitons will move away from the others. The critical value of the corresponding constants will be derived below with the condition $H_{\mathrm{V}}=0$.

Assume we have only periodic potential present and the initial soliton configuration is Eq. (4.1). For $A=0$ the solitons will go into an asymptotically free regime. Switching on the self-consistent periodic potentials (such that the solitons initially are located at its minima), it is natural to expect that for $A>A_{\mathrm{cr}}$ the solitons will be stabilized into a bound state. Then from the condition $H_{\mathrm{V}}=0$ we get

$$A_{\mathrm{cr}} = -\left(1-\frac{1}{N}\right)\frac{64\nu_0^4}{\pi\Omega}e^{-2\nu_0r_0}\sinh\frac{\pi\Omega}{4\nu_0}. \tag{5.23}$$

Note that the critical values generically should depend not only on the number of solitons N, but also on the initial configuration. The approach we used is not very sensitive to this. It cannot provide us with the intermediary critical values when the soliton train is stabilized after emitting two or more solitons.

We compared the theoretical predictions for A_{cr} from Eq. (5.23) with the data coming from the numeric solutions of the corresponding PCTC for different choices of the initial distance between the solitons r_0. The results are collected in Table I. The conclusion is that Eq. (5.23) provides correct dependence of A_{cr} on r_0 up to an overall constant factor of the order of 1.5.

In Table II we summarize two sets of critical values for the five-soliton trains. From our numeric experiment we derive two critical values of A. The first one, $A_{\mathrm{cr}}^{5,\mathrm{exp}}$, describes the value of A above which *all five solitons* form a bound state; the second one, $A_{\mathrm{cr}}^{3,\mathrm{exp}}$, shows the value of A above which the three middle solitons form a bound state while the two end ones separate.

TABLE II. The values of $A_{\rm cr}^{5,\rm exp}$ and $A_{\rm cr}^{3,\rm exp}$ obtained from numeric simulations with PCTC versus $A_{\rm cr}^{\rm th}$ obtained from Eq. (5.23) for $N=5$.

r_0	$A_{\rm cr}^{5,\rm exp}$	$A_{\rm cr}^{3,\rm exp}$	$A_{\rm cr}^{\rm th}$	$A_{5,\rm cr}^{\rm exp}/A_{\rm cr}^{\rm th}$	$A_{3,\rm cr}^{\rm exp}/A_{\rm cr}^{\rm th}$
2π	−0.0068	−0.0029	−0.0044	1.55	0.66
7	−0.0031	−0.0013	−0.0020	1.56	0.65
8	−0.00115	−0.00043	−0.00068	1.68	0.63
9	−0.00041	−0.000155	−0.00024	1.71	0.65

Again we see that formula (5.23) describes correctly the dependence of both critical values on r_0.

VI. CONCLUSIONS

We have studied the dynamics of an *N*-soliton train confined to external fields (quadratic, periodic, and tilted potentials). Both the analytical treatment in the framework of the PCTC model and numerical analysis by direct simulations of the underlying NLS equation show that the PCTC is adequate for description of the adiabatic *N*-soliton interactions in weak external potentials. A Hamiltonian approach for the perturbed NLS and CTC has been developed, and applied to the analysis of the soliton "expulsion" from the train, which is confined to a periodic potential.

As a physical system of direct relevance, we have considered matter-wave soliton trains in magnetic traps and optical lattices. In the range of parameters for the trapping potential, used in the BEC soliton train experiments, we found a good agreement between the analytical estimates based on the PCTC model and numerical simulations of the governing NLS equation. In what concerns the critical strength of the periodic potential at which the soliton expulsion occurs, analytical predictions qualitatively agree with numerical simulations. The developed theory can be useful for controlled manipulation with matter-wave soliton trains.

ACKNOWLEDGMENTS

V.S.G. and N.A.K. acknowledge partial support from the Bulgarian Science Foundation through Contract No. F-1410. B.B.B. wishes to thank the Department of Physics of the University of Salerno, Italy, for providing a research grant during which part of this work was done. M.S. acknowledges financial support from the MIUR, through the interuniversity project PRIN-2005 (Dynamical properties of Bose-Einstein condensates in optical lattices), and from the Istituto Nazionale di Fisica Nucleare, sezione di Salerno. We are grateful to Professor I. Uzunov for useful discussions and for calling our attention to Refs. [15,16].

[1] A. Hasegawa and Y. Kodama, *Solitons in Optical Communications* (Clarendon Press, Oxford, 1995).

[2] A. Barone and G. Paternó, *Physics and Applications of the Josephson Effect* (Wiley, New York, 1982).

[3] Y. Kivshar and G. Agrawal, *Optical Solitons: From Fibers to Photonic Crystals* (Academic Press, San Diego, 2003).

[4] B. B. Baizakov, B. A. Malomed and M. Salerno, Phys. Rev. A **70**, 053613 (2004);

[5] F. Kh. Abdullaev, A. Gammal, A. M. Kamchatnov, and L. Tomio, Int. J. Mod. Phys. B **19**, 3415 (2005); V. A. Brazhnyi and V. V. Konotop, Mod. Phys. Lett. B **18**, 267 (2004).

[6] For recent progress in theory and applications of BEC, see the special issue J. Phys. B **38**, No. (9) (2005).

[7] V. S. Gerdjikov, D. J. Kaup, I. M. Uzunov, and E. G. Evstatiev, Phys. Rev. Lett. **77**, 3943 (1996).

[8] V. S. Gerdjikov, I. M. Uzunov, E. G. Evstatiev, and G. L. Diankov, Phys. Rev. E **55**, 6039 (1997).

[9] J. M. Arnold, J. Opt. Soc. Am. A **15**, 1450 (1998); Phys. Rev. E **60**, 979 (1999).

[10] V. S. Gerdjikov, E. G. Evstatiev, D. J. Kaup, G. L. Diankov, and I. M. Uzunov, Phys. Lett. A **241**, 323 (1998).

[11] V. S. Gerdjikov and I. M. Uzunov, Physica D **152–153**, 355 (2001).

[12] V. S. Gerdjikov, *Complex Toda Chain—An Integrable Universal Model for Adiabatic N-soliton Interactions*, In Proceedings of the Workshop "Nonlinear Physics: Theory and Experiment. II," Gallipoli, 2002, edited by M. Ablowitz, M. Boiti, F. Pempinelli, and B. Prinari, pp. 64–70.

[13] V. S. Gerdjikov, On Modelling Adiabatic *N*-soliton Interactions. Effects of Perturbations, in *Nonlinear Waves: Classical and Quantum Aspects*, edited by F. Kh. Abdullaev and V. Konotop (Kluwer, Dordrecht, 2004), pp. 15–28.

[14] V. S. Gerdjikov, B. B. Baizakov, and M. Salerno, *Modelling Adiabatic N-soliton Interactions and Perturbations*, in Proceedings of the Workshop "Nonlinear Physics: Theory and Experiment. III," Gallipoli, 2004, edited by M. Ablowitz, M. Boiti, F. Pempinelli, and B. Prinari [Theor. Math. Phys. **144**, No. (2), 1138 (2005)]; V. S. Gerdjikov and B. B. Baizakov, *On Modelling Adiabatic N-soliton Interactions and Perturbations. Effects of External Potentials*, Report at the International Conference "Gravity, astrophysics and strings at the Black sea," Kiten, Bulgaria, June 10–16 (2004).

[15] S. Wabnitz, Electron. Lett. **29**, 1711 (1993).

[16] I. M. Uzunov, M. Gölles, and F. Lederer, J. Opt. Soc. Am. B **12**, 1164 (1995); I. M. Uzunov, M. Gölles, and F. Lederer, Phys. Rev. E **52**, 1059 (1995).

[17] K. E. Strecker, G. B. Partridge, A. G. Truscott, and R. G. Hulet, Nature (London) **417**, 150 (2002); K. E. Strecker *et al.*, Adv. Space Res. **35**, 78 (2005).

[18] A. Gammal, T. Frederico, and Lauro Tomio, Phys. Rev. A **64**, 055602 (2001).

[19] L. Khaykovich, F. Schreck, G. Ferrari, T. Bourdel, J. Cubizolles, L. D. Carr, Y. Castin, and C. Salomon, Science **296**, 1290 (2002).

[20] J. C. Bronski, L. D. Carr, B. Deconinck, J. N. Kutz, and K. Promislow, Phys. Rev. E **63**, 036612 (2001); Phys. Rev. Lett.

86, 1402 (2001); J. C. Bronski, L. D. Carr, R. Carretero-Gonzalez, B. Deconinck, J. N. Kutz, and K. Promislow, Phys. Rev. E **64**, 056615 (2001); F. Kh. Abdullaev, B. B. Baizakov, S. A. Darmanyan, V. V. Konotop, and M. Salerno, Phys. Rev. A **64**, 043606 (2001).

[21] R. Carretero-Gonzalez and K. Promislow, Phys. Rev. A **66**, 033610 (2002).

[22] V. I. Karpman and V. V. Solov'ev, Physica D **3**, 487 (1981).

[23] V. S. Gerdjikov, M. I. Ivanov, and P. P. Kulish, Theor. Math. Phys. **44**, No. (3), 342 (1980) (in Russian); V. S. Gerdjikov and M. I. Ivanov, Bulg. J. Phys. **10**, No. (1), 13–26 (1983); **10**, No. (2), 130–143 (1983) (in Russian).

[24] E. V. Doktorov, N. P. Matsuka, and V. M. Rothos, Phys. Rev. E **69**, 056607 (2004).

[25] Y. Kodama and A. Hasegawa, IEEE J. Quantum Electron. **QE-23**, 510 (1987).

[26] V. S. Shchesnovich and E. V. Doktorov, Physica D **129**, 115 (1999); E. V. Doktorov and V. S. Shchesnovich, J. Math. Phys. **36**, 7009 (1995).

[27] V. S. Gerdjikov, E. V. Doktorov, and J. Yang, Phys. Rev. E **64**, 056617 (2001).

[28] V. E. Zakharov, S. V. Manakov, S. P. Novikov, and L. P. Pitaevskii, *Theory of Solitons: The Inverse Scattering Method* (Plenum, New York, 1984).

[29] L. A. Takhtadjan and L. D. Faddeev, *Hamiltonian Approach to Soliton Theory* (Springer Verlag, Berlin, 1986).

[30] S. V. Manakov, Sov. Phys. JETP **67**, 543 (1974); H. Flaschka, Phys. Rev. B **9**, 1924 (1974).

[31] J. Moser, In *Dynamical Systems, Theory and Applications*. Lecture Notes in Physics Vol. 38 (Springer Verlag, Berlin, 1975), p. 467.

[32] V. S. Gerdjikov, E. G. Evstatiev, and R. I. Ivanov, J. Phys. A **31**, 8221 (1998).

[33] T. R. Taha and M. J. Ablowitz, J. Comput. Phys. **55**, 203 (1984).

[34] W. H. Press, S. A. Teukolsky, W. T. Vetterling, and B. P. Flannery, *Numerical Recipes. The Art of Scientific Computing* (Cambridge University Press, Cambridge, UK, 1996).

[35] B. P. Anderson and M. A. Kasevich, Science **282**, 1686 (1998).

[36] L. D. Carr and J. Brand, Phys. Rev. A **70**, 033607 (2004).

[37] V. S. Gerdjikov, Eur. Phys. J. B **29**, 237 (2002).

[38] D. Anderson and M. Lisak, Opt. Lett. **11**, 174 (1986).